Direct tip-position control using magnetic actuation for achieving fast scanning in tapping mode atomic force microscopy

G. R. Jayanth, Younkoo Jeong, and Chia-Hsiang Menq
Department of Mechanical Engineering, The Ohio State University, Columbus, Ohio 43202

(Received 22 November 2005; accepted 4 April 2006; published online 19 May 2006)

This article presents the development of a faster control loop for oscillation amplitude regulation in tapping mode operation of atomic force microscopy. Two techniques in relation to actuation and measurement are developed, that together significantly increase the bandwidth of the control loop. Firstly, magnetic actuation is employed to directly control the tip position of the cantilever to improve both the speed and the dynamics of the positioning system. Secondly, the signal path for oscillation amplitude regulation is separated from that for topography estimation in order to eliminate measurement delay that degrades the performance of the feedback loop. As a result, the phase-crossover frequency and gain margin of the control system are both increased, leading to a faster and more stable system. Two experiments are performed, one in air and the other in aqueous solution, to compare the developed control system with a commercial one and demonstrate the improvement. The results verify that the combination of the two techniques along with other existing methods eliminates all limitations associated with the instrument for the purpose of oscillation amplitude regulation, which is therewith dictated by the bandwidth of the cantilever. [DOI: 10.1063/1.2200874]

I. INTRODUCTION

In the tapping mode operation of atomic force microscopy (AFM), a cantilever is oscillated at its resonance frequency and controlled to gently tap the surface of a sample. The intermittent contact greatly reduces lateral force when compared with contact mode operation. The most commonly used method is a form of amplitude modulation, in which the oscillation amplitude of the cantilever is modulated by variations of the tip-to-sample distance. By feeding back changes in oscillation amplitude to adjust the cantilever z position, the amplitude is regulated at a set point while scanning a sample. The resulting changes in z position of a piezo-based positioner yields the topography of the sample surface. Faster changes in topography, which result from scanning the sample faster, necessitate faster response of the amplitude control system. Thus, while tapping mode AFM has found many applications,[1] the speed of the z-control loop has been one of the key barriers that limit imaging rate and inhibit innovation leading to new applications.

The dynamics of the z-control loop consists of several elements. Its response speed is directly related to the bandwidth of each element and is dictated by the slowest element in the loop. Some elements are connected with the instrument while others are related to the bandwidth of the cantilever and the tapping dynamics itself. In order to optimize the overall speed of the control loop, the speed of every element within the loop has to be optimized to match the fastest component in the feedback loop, which is usually the AFM cantilever. A key element connected with the instrument is the piezo-based z positioner whose bulky nature and underdamped dynamics severely restrict the closed-loop bandwidth even when other elements are significantly faster. Smaller piezopositioners increase positioning speed owing to correspondingly higher bandwidth, but at the cost of achievable z range.[2–4] In addition, the AFM has to be either custom designed or significantly modified to incorporate this feature. Integrated cantilevers with microfabricated piezoactuators[5,6] also solve this problem although practical considerations restrict the choice of the cantilever and its dynamical properties.[7] Two other significant factors that limit speed, namely, the bandwidth of tapping operation and the delay introduced by amplitude measurement with rms-to-dc converters, are decided by the bandwidth of the cantilever. Decreasing the quality factor using Q control increases the tapping bandwidth and alleviates the former problem,[8] but the latter issue has often limited the achievable speed of the control loop,[9] particularly when the bandwidth of the tapping dynamics and the speed of the z actuation have been improved.

In this article, two techniques in relation to actuation and measurement are developed, that together significantly increase the bandwidth of the control loop. Firstly, a magnetic actuator is proposed and implemented to directly control the position of the cantilever tip. The primary motivation for using magnetic actuation in tip-position control arises from the high bandwidth of this actuation technique and a significantly better dynamics of the actuator, namely, the actuation coil. In addition, virtually any cantilever can be modified to implement this technique. Although the magnetic actuator can also provide harmonic excitation to the cantilever, similar to that in MAC (magnetic ac) mode[10] operation, its purpose is to control the dc component of the tip position, not ac oscillation. Therefore, its design and implementation are different from those of usual MAC mode actuators. Secondly, the signal path for oscillation amplitude regulation is sepa-

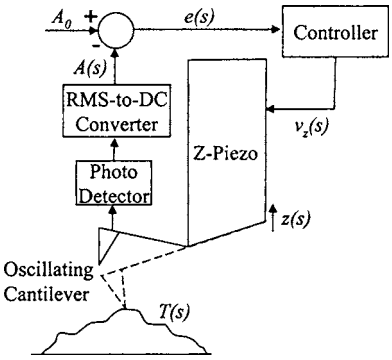

FIG. 1. A schematic showing the elements of a standard control system used in most commercial AFMs for oscillation amplitude regulation. The z-piezo, which is several centimeters long, is used to control the position of the cantilever during scanning.

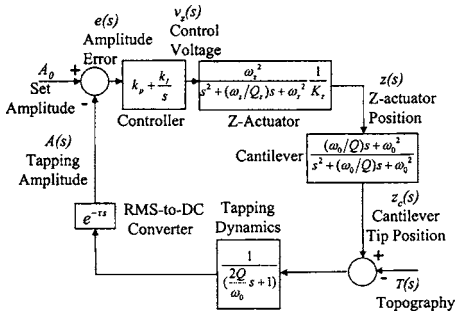

FIG. 2. A block diagram illustrating the dynamics of each element in the conventional amplitude control loop that uses z-piezo actuation and rms-to-dc conversion.

rated from that for topography estimation. This eliminates the rms-to-dc converter from the z control loop and its attendant time delay, thereby improving both the speed and stability of the control system.

Two experiments are performed, one in air and the other in aqueous solution, to compare the developed control system with a commercial one and demonstrate the improvement achieved in tracking fast-changing topography. The results verify that the combination of the two techniques along with other existing methods eliminates all limitations associated with the instrument for the purpose of oscillation amplitude regulation, which is therewith dictated by the bandwidth of the cantilever. The article has been divided into five parts. Section II discusses the principle of operation of the standard z-control loop and of the proposed modifications. Section III describes the experimental methods while Sec. IV discusses the results. Section V summarizes the advantages and flexibility of magnetic actuation-based z-position control.

II. PRINCIPLE OF OPERATION

A. Conventional control loop for oscillation amplitude regulation

Figure 1 is a schematic showing the elements of a standard control system used in most commercial AFMs for oscillation amplitude regulation. The principle of its operation is as follows: The cantilever is excited at resonance and controlled to tap the sample with amplitude A_0 which is close to its resonant amplitude. The sample topography $T(s)$, which changes as the sample is scanned, is a disturbance input to the amplitude control system. The effect of this disturbance is sensed as changes in the oscillation amplitude $e(s) = A_0(s) - A(s)$, which drives the z-piezo to change the position of the cantilever $z(s)$ to reject the effect of sample topography and restore the set oscillation amplitude A_0. If the disturbance rejection is perfect, $z(s)$ would equal $T(s)$, so topography is tracked perfectly. This is approximately valid at slow scan speeds and hence $z(s)$ is used to reconstruct the sample topography.

Figure 2 shows a block diagram to illustrate the dynamics of each element in this closed-loop control system. The cantilever taps the sample at its resonant frequency. The natural frequency of the cantilever $\omega_0/2\pi$ is typically in the range of 50–150 kHz. As the tapping cantilever is scanned over a surface, changes in topography excite transient dynamics in the cantilever and the tapping amplitude responds according to the dynamics of tapping operation.[7] Assuming no loss of tapping and no other energy dissipation besides that characterized by the quality factor Q, tapping dynamics can be approximately modeled with a first-order filter, whose bandwidth is limited to the value $\omega_0/2Q$. While the quality factor Q is dependent on the surrounding medium, it can also be controlled using a Q controller. In other words, tapping dynamics can be controlled using existing methods.

While scanning a sample, in order to acquire the necessary feedback signal to control the oscillation amplitude of the cantilever, a lock-in amplifier or a rms-to-dc converter is employed to yield a dc signal in proportion to the oscillation amplitude. The output signal of the converter is averaged over several multiples of the input period[7] so as to avoid leakage of the raw oscillation. This process introduces a corresponding measurement delay element ($e^{-\tau s}$) within the control loop.

A controller, typically of the proportional-integral type, is used to adjust the position of the cantilever, by moving a z-piezo upon which the cantilever is mounted, based on the discrepancy $e(s)$ between the measured amplitude and the set point. Due to the small bandwidth ($1-2$ kHz$=\omega_z/2\pi$) and underdamped nature of the z-piezo, more conservative choices of control gains are necessary to stabilize the control system. This problem is compounded by the existence of delay within the loop, which reduces the phase-crossover frequency and the gain margin. Thus, topography is tracked accurately only within a small closed-loop bandwidth.

B. Magnetic actuation for direct tip-position control

Previous applications of magnetic actuation in AFM include measurement of sample stiffness and dynamics,[11] Q control,[12] and providing ac excitation in tapping mode.[13] In this article, magnetic actuation is used to control z_c, the mean z position of the cantilever tip, by controlling the mean deflection of the cantilever. The principle of operation is based on torsional actuation,[12] wherein an orthogonal arrangement of the magnetic moment $\boldsymbol{m}$ of the cantilever and an external magnetic field $\boldsymbol{B}$ exert a torque $\boldsymbol{m}\times\boldsymbol{B}$ on the cantilever. If both these vectors are confined to the plane of motion of the cantilever, the torque $\tau=\boldsymbol{m}\times\boldsymbol{B}$ acts normal to this plane and

deflects the cantilever in proportion to its compliance. This deflection translates the cantilever tip along the z axis to the desired z position. A magnetic moment can be placed on the back surface of the cantilever tip either by coating the surface with a magnetic material[13] or by rigidly attaching a magnetic particle.[12]

A solenoid coil is used to generate the field $\boldsymbol{B}$ necessary to position the cantilever tip. The current through the coil exhibits first-order low-pass dynamics whose bandwidth is decided by the coil inductance L_c and the circuit resistance R. Thus, within the position-control loop, the second-order underdamped dynamics of the z-piezo is replaced by a more favorable first-order dynamics of the coil.

The actuation speed of this technique is decided by the bandwidth of the coil. This is determined by its physical characteristics including the wire diameter and the number of windings. In general, fewer windings result in smaller inductance L_c and correspondingly larger coil bandwidth, but at the cost of producing lesser magnetic field $\boldsymbol{B}$. This does not, however, result in serious trade off between actuation range and actuation speed. The actuation range also depends on the magnetic moment $\boldsymbol{m}$ of the cantilever and the current through the coil. Therefore, a higher actuation current and attachment of larger magnetic particles restore the necessary positioning range without sacrificing the coil bandwidth. Moreover, the coil inductance L_c itself can be actively changed to control the coil's bandwidth. With this flexibility, the application of direct tip-position control using magnetic actuation is not limited to conventional tapping mode operation of AFM. It can be used for other AFM applications and for any control techniques[14,15] that require fast actuators to regulate the z position of the cantilever.

C. Separation of signal paths for high-speed tip-position control

The process of rms-to-dc conversion improves the quality of topography reconstruction as it reduces leakage, and thus noise. However, it also results in measurement delay, which is detrimental to the stability and dynamic performance of the control system. Therefore, having a rms-to-dc converter in the control loop introduces a trade off between the speed of the control system and the image resolution of the microscope. Although the leakage signal is a spurious input to the system, its frequency is much higher than the closed-loop bandwidth of the control system. Therefore, the leakage signal widely separates in the frequency domain from the control signal of the z-position loop, and this renders the control system to be insensitive to this signal. These properties can be exploited to remove the process of signal averaging from the control loop while measuring the control signal to reconstruct topography after the leakage component is filtered *outside* the loop. In the absence of delay within the control loop, the phase-crossover frequency of the open-loop system is much higher, leading to a higher closed-loop bandwidth. This also increases the open-loop gain margin thereby increasing the stability of the control system.

Thus, the rms-to-dc converter is replaced by a simple full-wave rectifier within the control loop. The dc value of the rectifier's output is proportional to the oscillation amplitude. The higher frequency components are harmonics of cantilever oscillation beginning at twice its oscillation frequency. Hence, these harmonics are outside the bandwidth of even the fastest element of the control loop, the AFM cantilever, and well outside the closed-loop bandwidth of the control system. This is particularly valid when operating in air, where the high Q naturally limits the closed-loop bandwidth to a fraction of the cantilever bandwidth. In water, the advantage is lesser due to the low Q of the oscillating system, which results in a correspondingly high tapping bandwidth. Nevertheless, higher-order low-pass filters can be used in place of rms-to-dc conversion to attenuate the contribution of leakage and improve the performance over the existing control system. Separation of signal paths, therefore, removes the trade off between the speed of the control system and the image resolution of the microscope.

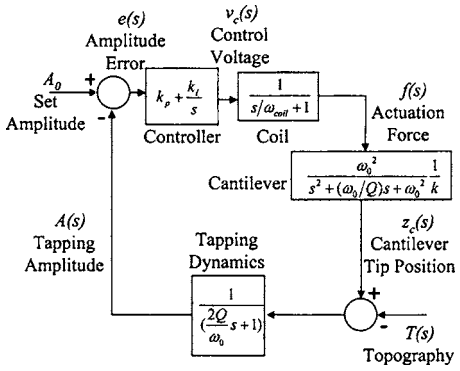

FIG. 3. A block diagram illustrating the direct tip-position control that uses magnetic actuation.

Figure 3 shows a block diagram of the closed-loop control system that uses magnetic actuation and feedback measurement as described in this section. The notable differences from Fig. 2 are in the replacement of a first-order transfer function for actuation and the absence of delay element arising from rms-to-dc conversion. In addition, since the magnetic actuation scheme is colocated with tip-position measurement, it does not introduce an open-loop zero in the transfer function of the cantilever.

III. EXPERIMENTAL METHODS

A. Experimental objective

In the closed-loop block diagram of the proposed control system (Fig. 3), the set point A_0 can be viewed as the reference signal and the topography $T(s)$ as the disturbance input to the control system. The control objective is to cancel the effect of this disturbance. Equivalently, topography $T(s)$ can be viewed as an unknown input, with the tip motion $z_c(s)$ being an estimate of the unknown topography. In the former case, the amplitude error $e(s)$ is a measure of the rejection of disturbance, while in the latter case $e(s)$ is related to the tracking error in tracking $T(s)$. Due to its importance as a useful measure in either case, the experimental objective was to measure $e(s)$ under the influence of $T(s)$ for the conventional and new control systems. This measurement was used to compare the performances of the two systems.

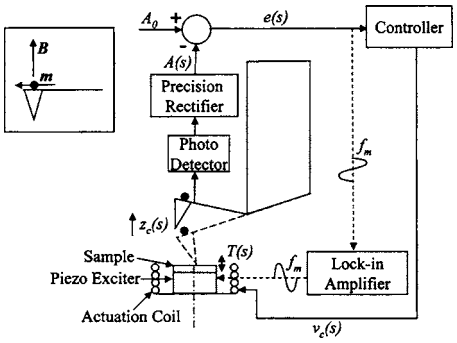

FIG. 4. A schematic of the experimental setup which was used to control the tapping amplitude and evaluate its performance.

B. Cantilever preparation for magnetic actuation

A permanent magnet particle was attached on the cantilever surface at the back of the cantilever tip in order to control its position. A samarium cobalt permanent magnet (Culver City Hardware, CA) was crushed and a particle, about 20 μm in size, was attached using epoxy to the end of the cantilever (NSC35/AlBS, MikroMasch) by means of suitable micromanipulators.[11] The amount of epoxy and the size of the particle were both small, leaving a major part of the cantilever surface available to focus the measurement laser beam. Before the epoxy set, a strong permanent magnet was used to align the magnetic moment of the particle along the length of the cantilever. This ensured that the magnetic moment was roughly orthogonal to the vertically directed magnetic field $\boldsymbol{B}$ generated by a solenoid (Fig. 4, inset), so the torque experienced by the cantilever was maximum. Secondly, this also guaranteed that the torque acts normal to the plane of deflection of the cantilever and actuates the cantilever in the z direction. Since particle attachment increased the motional mass of the cantilever, its natural frequency dropped to 50–70 kHz from its nominal value of 150 kHz, and the Q in air was around 500.

One of the primary concerns about this technique is the potential for contamination of the cantilever tip during particle attachment.[16] In order to test the quality of the tip, the interaction force versus distance curve of a new cantilever was generated on freshly cleaved mica and compared with the curve generated after the particle was attached. No significant difference was found between the two curves, testifying to the acceptable quality of the tip even after the attachment.

C. Demodulation of the cantilever oscillation to measure the amplitude

The raw oscillation signal of the cantilever was first high-pass filtered to eliminate dc offset and drift and allow only the cantilever oscillation. This oscillation signal was rectified by means of a precision full-wave rectifier.[17] The full-wave rectifier exactly doubles the frequency of this input sinusoid and therefore pushes it outside the bandwidth of the AFM cantilever. A fourth-order low-pass filter (model 3202R, Krohn-Hite) was cascaded with the rectifier and used to measure the dc value of the rectified signal, which is proportional to the oscillation amplitude. The cutoff frequency of the filter was sufficiently high as to not introduce any significant delay into the control system, but sufficiently low as to attenuate the harmonics at the output of the rectifier. Since the experiments were conducted with two cantilevers whose natural frequencies were in the range of 50–70 kHz, the low-pass filter cutoff was set in the range of 20–30 kHz.

D. Simulation of topography

The advantages of the proposed changes to the control loop were evident in the frequency domain description as the increase in the phase-crossover frequency and gain margin of the open-loop system. Thus, the control systems were also compared in the frequency domain by providing a sinusoidal topographic disturbance $T(j2\pi f_m)$ and recording the error $e(j2\pi f_m)$ as a function of the "topographic frequency" f_m. Since the control system is sensitive only to changes in the gap between the tapping cantilever and the sample, the topography T was simulated by changing the absolute position of one of them, typically by few nanometers. In the first method, magnetic actuation was used to change the mean position of oscillation of the cantilever using an external sinusoidal input. This modulated the cantilever-sample gap while the cantilever tapped at a fixed point on the sample, and simulated sinusoidal topography. The second method was realized by mounting the sample on a commercial piezoexciter (CMA-P4, Noliac Inc.) whose position was sinusoidally changed, thereby modulating the cantilever-sample gap. In either experiment, a commercial lock-in amplifier (model 7280, Perkin Elmer) provided the necessary sinusoidal voltage input and measured the amplitude-error $e(j2\pi f_m)$ at each frequency f_m. The topographic frequency f_m was swept over a wide range to study the dynamics of disturbance rejection.

This technique also added flexibility in choosing the sample and the height of topography unlike scanning a grating, which constrains the test wave form (usually to a nonsinusoidal one), its amplitude, and the sample material.

A schematic of the magnetically actuated control system is shown in Fig. 4. A centimeter-sized coil generates vertically directed magnetic field $\boldsymbol{B}$. The inset shows the approximate relative orientations of the magnetic moment $\boldsymbol{m}$ of the attached particle and the magnetic field $\boldsymbol{B}$ of the coil. Figure 5 shows photographs of the experimental arrangement and a micrograph of the cantilever.

IV. RESULTS

All experiments were performed using a Molecular Imaging PicoPlus™ AFM.

A. Elimination of measurement delay

Elimination of measurement delay comprises an important aspect of improvements to the proposed control loop. This is demonstrated by measuring the transfer function for tapping dynamics in Fig. 3. In conventional systems, this is cascaded with the measurement delay introduced by the rms-to-dc converter (Fig. 2). Thus, a linearly decreasing phase lag due to the delay[18] is superposed on the actual phase response

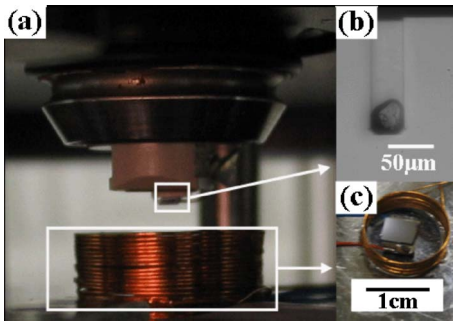

FIG. 5. (Color online) Photographs showing the important components in the experiment: (a) the actuation coil positioned beneath the z-positioner nose cone within the AFM. (b) A micrograph of the back surface of the cantilever showing the magnetic particle attached at its end. (c) The SiO_2 sample, mounted on the piezoexciter and positioned within the actuation coil.

of the tapping dynamics. Replacement of the rms-to-dc converter with a precision rectifier enables extraction of the true phase response of this transfer function.

To measure the tapping dynamics, the amplitude control system was switched off during the experiment and changes in tapping amplitude were recorded under the influence of sinusoidal topographic input. The amplitude of the input $T(j2\pi f_m)$ was 2–3 nm and was realized using the first method described in Sec. III D, wherein the mean tapping position z_c of the cantilever was magnetically changed at frequency f_m. The phase lag of the sinusoidal response of the tapping amplitude $A(j2\pi f_m)$ was measured at the output of the rms-to-dc converter and the precision rectifier, respectively. They are plotted together in Fig. 6 as functions of f_m. The phase response measured at the output of the rectifier clearly demonstrates a change of approximately 90° across the tapping bandwidth, in accordance with the predicted first-order model for tapping dynamics. The slight droop in the phase beyond 10 kHz is from the low-pass filter cascaded with the rectifier. The linearly decreasing phase contributed by the rms-to-dc converter appears as an exponentially increasing phase lag in the log-frequency phase plot and obscures the true phase response of tapping dynamics. The corresponding measurement delay τ of 0.62 ms results in a phase-crossover frequency of 800 Hz, which also limits the

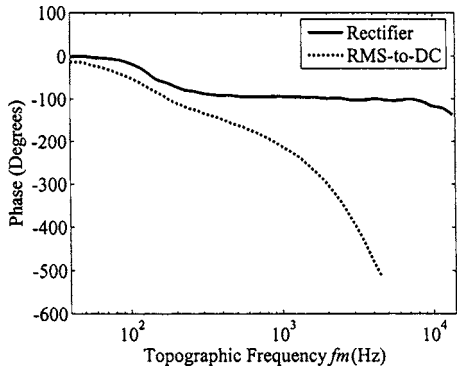

FIG. 6. The phase lag of amplitude variations with respect to the topographic variations as a function of topographic frequency f_m. In the experiment, the cantilever was acoustically excited in air at its resonance of 50.3 kHz to amplitude around 100 nm and set to tap a SiO_2 sample at 95% of its resonant amplitude.

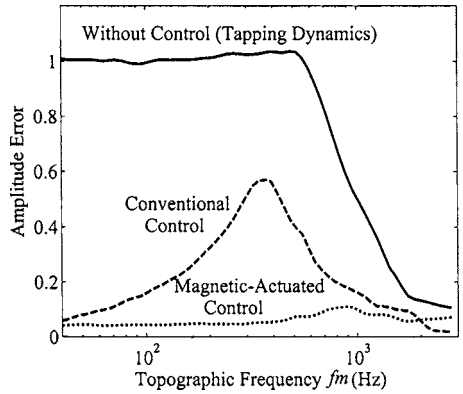

FIG. 7. Performances of the two control systems in suppressing amplitude error $e(j2\pi f_m)$ in air arising from topographic changes $T(j2\pi f_m)$. The conventional controller was tuned to an integral gain of 1% and a proportional gain of 25%. The magnetic control loop used a lag compensator with a pole at 600 Hz, zero at 3 kHz, and a dc gain of 25. The resonant frequency of the cantilever was 50.3 kHz, and tapping amplitude was ~100 nm.

control bandwidth to this value in closed loop.

B. Comparison of control performances in air

The experiments in air were designed to highlight the limitations primarily from components of the control loop other than the tapping dynamics. To this end, Q control was used to widen the tapping bandwidth and minimize its influence by reducing the Q of the cantilever to 125.[12,19] Before performing the experiment, the conventional controller's proportional and integral gains were tuned to their optimal best beyond which its control system displayed instability. The topography was simulated using the second method described in Sec. III D, wherein a SiO_2 sample was mounted on a piezoactuator and vibrated at f_m with an amplitude of 2–3 nm. The magnetically actuated control loop employed a lag compensator as the controller which was built using MATLAB® and SIMULINK™ and implemented in DS1104 (dSPACE Inc.) real-time controller. The location of the pole, zero, and the dc gain of the controller reported here corresponds to the best response measured with several different settings. The actuation bandwidth of the coil was set to around 20 kHz by appropriately choosing the circuit resistance. The amplitude error $e(j2\pi f_m)$ was measured at the output of the respective measurement devices for each control loop, namely, rectifier and rms-to-dc converter.

A preliminary measurement was made without amplitude control to read out the tapping dynamics. This was normalized to unity within the tapping bandwidth and represents amplitude variation without position control. Figure 7 compares the performances with the two control systems in operation. The proposed system suppresses amplitude error $e(j2\pi f_m)$ almost uniformly to 4% of the uncontrolled variation at all frequencies f_m within the tapping bandwidth. The performance of the conventional control loop is comparable to this at low frequencies (i.e., for slow changes in topography). However, the error increases with increasing frequency f_m and the amplitude variation at 400 Hz is 55% of the uncontrolled value. Equivalently, while the proposed system uniformly demonstrates 4% error in tracking topography, the conventional system demonstrates significantly higher error

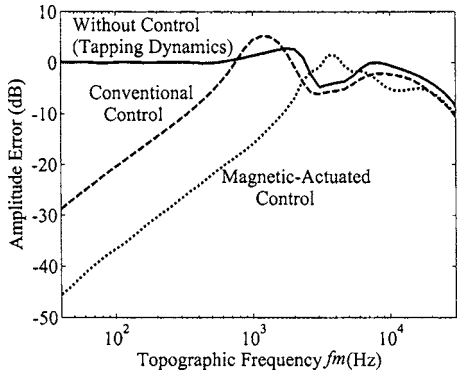

FIG. 8. Performances of the two control systems in suppressing amplitude error $e(j2\pi f_m)$ in water arising from topographic changes. The conventional controller was tuned to an integral gain of 0.7% and a proportional gain of 0.048%. The magnetic control loop used low-pass filter to approximate an integrator. The filter cutoff was set to 10 Hz and the open loop gain was 360. The resonant frequency of the cantilever was 69 kHz and tapping amplitude was ~100 nm.

for faster topography. Since both control systems were tuned to achieve the greatest possible rejection of topographic disturbance, the difference in performance is a result of the intrinsic limitations imposed by the bandwidth of the components of the conventional system.

C. Comparison of control performances in aqueous solution

Tracking performance in aqueous medium was compared with a similar experiment as described above. However, the Q of the cantilever in water was 7, so that the tapping bandwidth was more than 10% of the cantilever's bandwidth. This was comparable to the bandwidth of the measurement scheme of the new system. This resulted in inclusion of phase lag from the low-pass filter that was cascaded with the rectifier, thereby reducing the gain margin. Integral control was therefore employed to increase the gain margin. To avoid problems such as integrator wind up, a low pass filter with very low cut-off frequency was used instead of an actual integrator.

Due to the wider closed-loop bandwidth of the control system, larger disturbance rejection was achieved at low frequencies. Thus, a log-log plot is used to compare the tracking errors $e(j2\pi f_m)$ (Fig. 8). The amplitude error e due to topographic variation T without amplitude control is normalized to unity (0 dB) within the tapping bandwidth as before. Since both the controllers employ integral control, the error increases with frequency at 20 dB/decade. However, the tracking error achieved by magnetic control is over 16 dB (6.3 times) lesser than the error achieved by the conventional system within the tapping bandwidth. This once again reflects the improved ability of the proposed control system in rejecting high-frequency topographic disturbance.

V. DISCUSSION

The experimental results demonstrate that the proposed system tracks fast-changing topography significantly better than the conventional control system both in air and in aqueous medium. This is directly the result of simultaneously improving the bandwidths of all the key elements of the control loop. The proposed methods solve two of the three key limitations of conventional systems, namely, actuator dynamics and measurement delay. Existing methods for Q control address the final limitation due to the tapping dynamics.

Since the bandwidth of the z-control loop is now decided by the bandwidth of the actuation coil, it is still a property of the instrument. A useful feature of magnetic actuation is that the inductance of the coil can be actively changed using current feedback to modify the bandwidth of the actuation circuit (see Appendix). This can be used to customize the coil bandwidth to any cantilever that is chosen to operate with. Large changes in bandwidth are easily achieved with relatively small control efforts. On the other hand, the high stiffness, second-order dynamics, and low sensitivity of the z-piezo impose theoretical limitations to changes in its bandwidth and practical challenges to realize them due to the necessary high voltages.

Hence, the combination of magnetic actuation, Q control, and elimination of delay removes all limitations associated with the instrument for the purpose of oscillation amplitude regulation. It improves the control system speed, which is therewith dictated by the bandwidth of the cantilever.

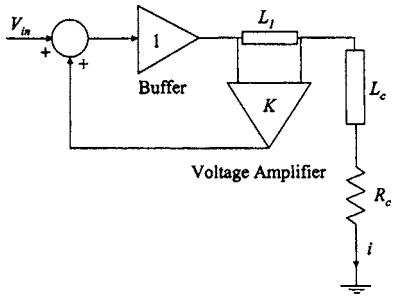

FIG. 9. A circuit diagram of the technique used to actively tune the coil bandwidth.

ACKNOWLEDGMENTS

This material is based on work supported by the National Science Foundation under Grant No. BES-0421273. Any opinions, finding, conclusions, or recommendations expressed in this material are those of the authors and do not necessarily reflect the views of the National Science Foundation.

APPENDIX: TECHNIQUE TO ACTIVELY TUNE ACTUATION BANDWIDTH

A home designed and built circuit is discussed here to achieve flexibility by actively controlling the bandwidth of the actuation coil. The original coil is modeled by its inductance L_c and resistance R_c. Another coil of impedance L_1 is added in series and the potential difference across its ends is amplified by a factor K and fed back (Fig. 9). For an externally applied voltage V_{in} the circuit current i obeys the following equation:

$$V_{\text{in}} = [L_c - (K-1)L_1]\frac{di}{dt} + R_c i.$$

Thus, the effective inductance of the circuit is $L_c-(K-1)L_1$. For stability of the closed-loop system, we require $(K-1)L_1<L_c$. For $K>1$ the effective inductance is less than L_c, thereby reducing the time constant of the circuit. The dc gain of the coil is decided by R_c, which remains the same. While the experiments reported in this article did not necessitate the use of this technique, separate tests easily achieved tenfold improvement in the coil bandwidth, although significant second-order behavior of the closed-loop system was noticed for higher feedback gain K. This was probably due to the unmodeled output capacitance of the feedback operational amplifiers.

[1] R. Garcia and R. Perez, Surf. Sci. **47**, 197 (2002).
[2] T. Ando, N. Kodera, Y. Naito, T. Kinoshita, K. Furuta, and Y. Y. Toyoshima, ChemPhysChem **4**, 1196 (2003).
[3] T. Ando, N. Kodera, E. Takai, D. Maruyama, K. Saito, and A. Toda, Proc. Natl. Acad. Sci. U.S.A. **98**, 12468 (2001).
[4] N. Kodera, H. Yamashita, and T. Ando, Rev. Sci. Instrum. **76**, 053708 (2005).
[5] S. R. Manalis, S. C. Minne, A. Atalar, and C. F. Quate, Rev. Sci. Instrum. **67**, 3294 (1996).
[6] S. C. Minne, S. R. Manalis, and C. F. Quate, *Bringing Scanning Probe Microscopy Up To Speed* (Kluwer, Massachusetts, 1999).
[7] T. Sulchek, G. G. Yaralioglu, C. F. Quate, and S. C. Minne, Rev. Sci. Instrum. **73**, 2928 (2002).
[8] T. Sulchek *et al.*, Appl. Phys. Lett. **76**, 1473 (2000).
[9] B. Rogers *et al.*, Rev. Sci. Instrum. **74**, 4683 (2003).
[10] http://www.molec.com/products_options.html#products_macmode
[11] E. L. Florin, M. Radmacher, B. Fleck, and H. E. Gaub, Rev. Sci. Instrum. **65**, 639 (1994).
[12] J. L. Garbini, K. J. Bruland, W. M. Dougherty, and J. A. Sidles, J. Appl. Phys. **80**, 1959 (1996).
[13] W. Han, S. M. Lindsay, and T. Jing, Appl. Phys. Lett. **69**, 4111 (1996).
[14] D. R. Sahoo, A. Sebastian, and M. V. Salapaka, Appl. Phys. Lett. **83**, 5521 (2003).
[15] Y. Jeong, G. R. Jayanth, and C.-H. Menq, Appl. Phys. Lett. (to be published).
[16] B. Rogers, D. York, N. Whisman, M. Jones, K. Murray, J. D. Adams, T. Sulchek, and S. C. Minne, Rev. Sci. Instrum. **73**, 3242 (2002).
[17] http://sound.westhost.com/appnotes/an001.htm
[18] G. F. Franklin, J. D. Powell, and A. Emami-Naeini, *Feedback Control of Dynamic Systems*, 4th ed. (Prentice Hall, New Jersey, 2002).
[19] H. Holscher, Surf. Sci. **515**, 517 (2002).